© 2017. Published by The Company of Biologists Ltd | Journal of Experimental Biology (2017) 220, 1709-1720 doi:10.1242/jeb.153858

RESEARCH ARTICLE

The sphingosine rheostat is involved in the cnidarian heat stress response but not necessarily in bleaching

Sheila A. Kitchen‡,* and Virginia M. Weis

ABSTRACT

Sphingolipids play important roles in mitigating cellular heat and oxidative stress by altering membrane fluidity, receptor clustering and gene expression. Accumulation of signaling sphingolipids that comprise the sphingosine rheostat, pro-apoptotic sphingosine (Sph) and pro-survival sphingosine-1-phosphate (S1P) is key to determining cell fate. Reef-building corals and other symbiotic cnidarians living in shallow tropical waters can experience elevated seawater temperature and high UV irradiance, two stressors that are increasing in frequency and severity with climate change. In symbiotic cnidarians, these stressors disrupt the photosynthetic machinery of the endosymbiont and ultimately result in the collapse of the partnership (dysbiosis), known as cnidarian bleaching. In a previous study, exogenously applied sphingolipids altered heat-induced bleaching in the symbiotic anemone *Aiptasia pallida*, but endogenous regulation of these lipids is unknown. Here, we characterized the role of the rheostat in the cnidarian heat stress response (HSR) and in dysbiosis. Gene expression of rheostat enzymes sphingosine kinase (*AP-SPHK*) and S1P phosphatase (*AP-SGPP*), and concentrations of sphingolipids were quantified from anemones incubated at elevated temperatures. We observed a biphasic HSR in *A. pallida*. At early exposure, rheostat gene expression and lipid levels were suppressed while gene expression of a heat stress biomarker increased and 40% of symbionts were lost. After longer incubations at the highest temperature, *AP-SGPP* and then Sph levels both increased. These results indicate that the sphingosine rheostat in *A. pallida* does not participate in initiation of dysbiosis, but instead functions in the chronic response to prolonged heat stress that promotes host survival.

KEY WORDS: *Aiptasia pallida*, Symbiodinium, Sphingolipids, Coral bleaching

INTRODUCTION

Many cnidarians, such as corals and sea anemones, engage in endosymbiotic associations with photosynthetic dinoflagellates in the genus *Symbiodinium* spp. These partnerships are the centerpiece of coral reef ecosystems and are severely threatened by abiotic stressors associated with climate change, especially elevated temperature (Hoegh-Guldberg et al., 2007). The algal photosynthetic apparatus is sensitive to climate-induced heat and light perturbations, which result in photosystem dysfunction (Warner et al., 1996), and increased reactive oxygen and nitrogen species (ROS and RNS) generation in the algae (Hawkins and Davy, 2012; Lesser, 1996; McGinty et al., 2012) and in turn oxidative stress in the host (Hawkins et al., 2014; Perez and Weis, 2006; Richier et al., 2006). Symbiotic cnidarians have protective mechanisms including heat shock proteins (Hsps), oxygen-scavenging enzymes and fluorescent proteins to reduce the effects of moderate fluctuations in heat and light exposure (Louis et al., 2017; Venn et al., 2008). However, during prolonged heat or light stress, these stress mechanisms can become overloaded, ultimately leading to a massive loss of symbionts, or dysbiosis, from cnidarian hosts, resulting in cnidarian bleaching. Although there have been extensive studies on dysbiosis in a variety of corals and sea anemone model systems (reviewed by Weis, 2008), our understanding of the cellular events preceding symbiont loss is limited. Given that lipids are co-directors of phagocytosis (Heung et al., 2006; Steinberg and Grinstein, 2008), the mode by which *Symbiodinium* are acquired by hosts, dysbiosis could have significant impacts on lipid signaling, targeting and trafficking events.

Oxidative and heat stress are two cellular events mediated by bioactive sphingolipids in both eubacterial and eukaryotic cells (An et al., 2011; Jenkins et al., 1997; van Brocklyn and Williams, 2012). The lipid messengers sphingosine (Sph) and sphingosine-1-phosphate (S1P) have antagonistic roles in the cell, where Sph initiates programmed cell death pathways while S1P activates cell survival and proliferation (Le Stunff et al., 2004; Olivera and Spiegel, 2001; Spiegel and Milstien, 2003). The enzymatic activities of sphingosine kinase (SPHK) and sphingosine-1-phosphate phosphatase (SGPP) maintain the homeostatic balance of these sphingolipids in this so-called ‘sphingosine rheostat’ (Cuvillier et al., 1996; Mandala et al., 1998). Heat stress studies in mammalian cell lines, yeast and gut microbiome commensals *Bacteroides* suggest an evolutionarily conserved sphingolipid-mediated heat stress response (HSR) (An et al., 2011; Chang et al., 1995; Jenkins et al., 2002, 1997). The HSR is a defense mechanism controlled by stress sensors and signal transduction pathways to offset the deleterious effects of thermal stress (Hofmann and Todgham, 2010). In yeast and *Bacteroides*, elevated temperatures decreased cell viability in sphingolipid-deficient strains, and this was rescued with sphingolipid supplementation. Furthermore, in yeast and mammalian cells, synthesis of Sph and its precursor ceramide increased with heat stress (Chang et al., 1995; Jenkins et al., 1997). Elevated Sph levels were reversed in yeast by deletion of the SGPP-like enzyme, which increased the cellular S1P-like metabolites, thereby enhancing survival (Mandala et al., 1998; Mao et al., 1999).

Oxidative stress is also linked to the sphingosine rheostat through modulation of S1P levels in yeast (Lanterman and Saba, 1998), nematodes (Deng et al., 2008), fruit flies (Kawamura et al., 2009), fish (Yabu et al., 2008) and mammals (Ader et al., 2008; Gomez-Brouchet et al., 2007; Pchejetski et al., 2007). The

Department of Integrative Biology, Oregon State University, 3029 Cordley Hall, Corvallis, OR 97331, USA.
*Present Address: Department of Biology, Pennsylvania State University, 208 Mueller Laboratory, State College, PA 16802, USA.

‡Author for correspondence (kitchens.osu@gmail.com)

S.A.K., 0000-0003-4402-8139

Received 27 November 2016; Accepted 16 February 2017

Journal of Experimental Biology (2017) 220, 1709-1720 doi:10.1242/jeb.153858

rheostat response is dependent on the severity of oxidative damage, with moderate ROS levels activating SPHK and increasing S1P levels (Ader et al., 2008), while severe ROS levels degrade SPHK, reduce S1P and shift cells toward death (Gomez-Brouchet et al., 2007; Pchejetski et al., 2007). Furthermore, the activation of the Hsp90–endothelial NOS (eNOS) protein complex by S1P causes production of an RNS, cytotoxic nitric oxide (NO), which at low cellular levels can inhibit pro-inflammatory cytokines (De Palma et al., 2006; García-Cardeña et al., 1998) (Fig. 1A). In contrast, immune elicitors and elevated ROS trigger inducible NOS, resulting in high cellular NO and NO-dependent elevations in ceramide through activation of lysosomal acidic sphingomyelinases (A-SMase) (Perrotta et al., 2008) (Fig. 1B). Ceramides then assemble with cholesterol to form ceramide-rich rafts in cellular and organellar membranes, altering membrane fluidity and cell signaling toward cell death (Balogh et al., 2013). These findings suggest an active role for the sphingosine rheostat in the cellular stress response, and led Maceyka and coworkers (2007) to propose SPHK as a central enzyme in the oxidative stress pathway in mammals. Its importance in the invertebrate stress response, however, requires further investigation.

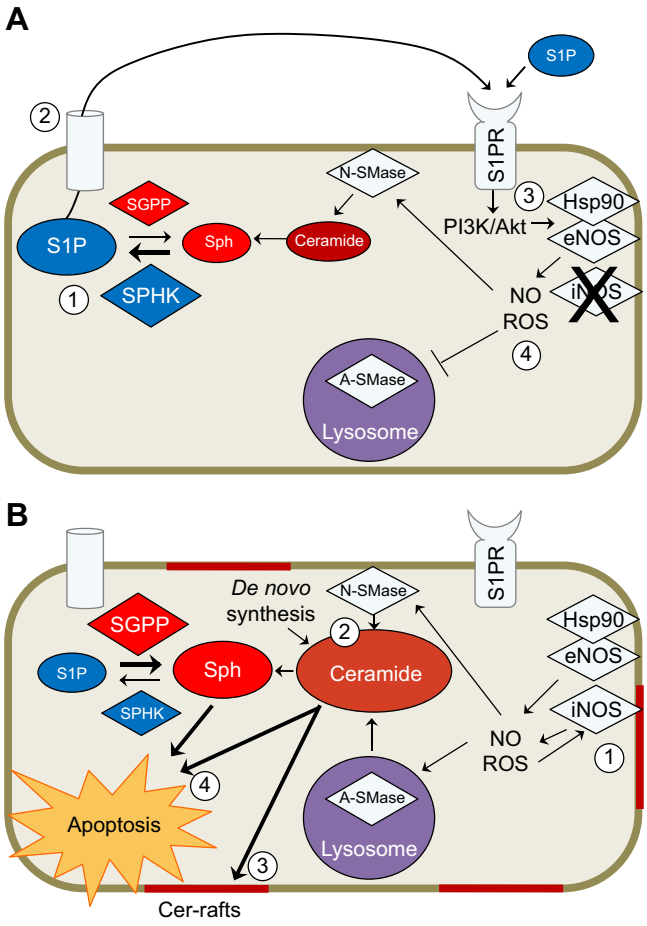

Fig. 1. Model for mammalian sphingosine rheostat under heat stress. (A) Under a moderate stress event, the rheostat shifts toward upregulation of sphingosine kinase (SPHK) and increased pro-survival sphingosine-1-phosphate (S1P) (1). S1P can be exported and initiate receptor-mediated cell signaling through the S1P receptor (SIPR) (2), which activates the PI3K/Akt pathway (3), which in turn activates the heat shock protein 90 (Hsp90)–endothelial nitric oxide synthase (eNOS) complex, resulting in low constitutive nitric oxide (NO) production (4) that promotes cellular neutral sphingomyelinase (N-SMase) activity but inhibits acidic sphingomyelinase (A-SMase) activity in the lysosome. These cellular events result in a pro-survival signaling of the rheostat to return to homeostasis. (B) Under a high heat stress event, higher cytosolic levels of reactive oxygen species (ROS) and NO, from the increased activity of the Hsp90–eNOS heterocomplex and stimulation of inducible NOS (iNOS), activate N-SMase, lysosomal A-SMase and *de novo* ceramide synthesis to increase cellular ceramide (2). Ceramide accumulation leads to the formation of ceramide-rich lipid platforms (3), and shifts the sphingosine rheostat towards cell death (4).

In symbiotic cnidarians, the molecular crosstalk between the host and symbionts during dysbiosis is still only partially understood. In stable associations, symbionts are housed in host-derived vesicles, or symbiosomes, that resist phagosomal maturation (Chen et al., 2004, 2003, 2005). Transcriptional studies on symbiotic cnidarians exposed to elevated temperature or high irradiance stress indicate that symbiont removal mechanisms such as host apoptosis, innate immunity and exocytosis are upregulated (DeSalvo et al., 2008; Richier et al., 2006; Starcevic et al., 2010). Modulation of sphingolipids could underlie these changes through activation of phagosomal maturation (Heung et al., 2006) and cell death (Maceyka et al., 2002). The cnidarian sphingosine rheostat has been implicated in symbiosis maintenance (Hemond et al., 2014; Rodriguez-Lanetty et al., 2006), immunity and the HSR (Detournay and Weis, 2011). In the sea anemone *Aiptasia pallida* (also known as *Exaiptasia pallida*; Grajales and Rodriguez, 2014), exposure to an elevated temperature with the addition of exogenous Sph increased algal loss by 40%, whereas incubation in exogenous S1P reduced bleaching by nearly 50% (Detournay and Weis, 2011). Moreover, elevated Sph led to increased host caspase activity, an indicator of programmed cell death. However, cytotoxic NO production, implicated in symbiosis breakdown (Hawkins et al., 2013; Perez and Weis, 2006; Ross, 2014) and functionally coupled to sphingolipid metabolism in other systems (Perrotta et al., 2008), was unaffected by Sph and S1P (Detournay and Weis, 2011).

Given that exogenous sphingolipids altered the amount of symbiont loss and host cell death in *A. pallida* during heat stress, we predicted that endogenous transcriptional regulation of rheostat enzymes (AP-SPHK and AP-SGPP) and concomitant changes in sphingolipid metabolites contribute to the initiation of dysbiosis and a host HSR. The sea anemone *Aiptasia* sp. is a widely used model system for the study of coral symbiosis physiology and cell biology (Goldstein and King, 2016; Weis et al., 2008). Its ease of culture, rapid growth rate and well-developed genomic resources (Baumgarten et al., 2015; Lehnert et al., 2012) make it a valuable resource for empirical studies of symbiosis that cannot be carried out in corals. In this study, we experimentally examined the response of the host sphingosine rheostat to elevated temperature through time by quantification of *AP-SPHK*, *AP-SGPP* and HSR biomarker *Hsp90* gene expression, sphingolipid concentrations and symbiont loss over a prolonged heat stress lasting 7 days.

MATERIALS AND METHODS

Maintenance of *A. pallida* and *Symbiodinium* cultures

Symbiotic *A. pallida* (Agassiz in Verrill 1864) from the Weis Lab population (VWA; Grajales and Rodríguez, 2016) were maintained in artificial seawater (ASW) at room temperature (RT, ~25°C) under 40 µmol quanta m^{-2} s^{-1} intensity on a 12 h light:12 h dark photoperiod to promote symbiont photosynthesis and proliferation. Anemones were fed *Artemia* sp. nauplii twice a week up to 2 weeks prior to the commencement of experiments, after which time they were starved. The symbionts, *Symbiodinium minutum* strain CCMP830 (type B1, Bigelow Laboratory for Ocean Science, East Boothbay, ME, USA) previously isolated from *A. pallida* (Lesser,

Journal of Experimental Biology (2017) 220, 1709-1720 doi:10.1242/jeb.153858

1996), were grown in sterile f/2 media (Guillard and Ryther, 1962) at 25°C at an irradiance of 40 µmol quanta m^{-2} s^{-1} on a 12 h light:12 h dark cycle.

Elevated temperature treatment of *A. pallida*

Anemones were randomly placed into 6-well plates (for qPCR, three anemones per well; for lipid analyses, one anemone per well) with 10 ml of 0.45 µm-filtered artificial seawater (FASW) 1 week prior to treatment. During the 2 weeks before and throughout the week of temperature exposure, the anemones were starved, given daily FASW changes and any expelled symbionts were removed. All experiments were carried out in temperature-controlled incubators. For the qPCR assay, anemones were exposed to a range of temperatures – 25 (ambient), 27, 30 and 33°C – for 1 week. Anemones were sampled at 0.5, 1, 2, 4 and 7 days (n=3 per time point). Additional samples were collected at 3 and 6 h for ambient and 33°C to investigate early expression differences at these experimental temperatures. The intermediate elevated temperatures (27 and 30°C) did not result in detectable gene expression differences (see Results); therefore, only ambient and 33°C-treated anemones were used for quantification of sphingolipids. Anemones were sampled over two experiments, at 1, 4 and 7 days in experiment 1 (n=4) and 6 h and 7 days in experiment 2 (n=10) based on gene expression results. At designated time points, anemones were rinsed in FASW before being frozen in liquid nitrogen and stored at −80°C until processed for qPCR or sphingolipid extraction.

Bleaching quantification

To quantify symbiont loss from host tissues during exposure to elevated temperature, symbiont chlorophyll autofluorescence was measured from the set of anemones that were destined for lipid analysis. Measurements were taken from each individual until they were killed at their designated time point. First, each anemone was imaged under white light on the Zeiss Stemi 2000-c stereo-microscope (Zeiss, Oberkochen, Germany) with standardized camera settings and 1 s exposure to determine well location and measure oral disc size. Autofluorescence was then detected using a long-pass emission filter (>665 nm) and digitally captured with a 25 s camera exposure after excitation by 470 nm LED blue light at 130 µmol quanta m^{-2} s^{-1} intensity. Mean fluorescence intensity for each individual at each time point was measured from 10 random areas of the oral disc or base of the tentacles using ImageJ v1.47 software (Rasband, 1997-2015). Autofluorescence was normalized to the mean fluorescence intensity from five areas adjacent to the anemones considered to be background levels. The random effect of repeated measures of autofluorescence from the same individual was significant in the generalized linear mixed-effects model (GLMM; Chi-square goodness of fit test, P<0.001), but not the well position in the plate. Therefore, normalized values were fitted with a GLMM model with fixed effects of time (continuous) and temperature (factor, two levels), and random effect of sample. Anemone size was estimated by their amount of total protein, a common proxy for *A. pallida* size in hyperthermal experiments (Bieri et al., 2016; Goulet et al., 2005; Sunagawa et al., 2008). For each sample, total protein was quantified using a Bradford assay from a 100 µl aliquot of the homogenized tissue from the lipid extraction described below. To determine whether host size affected the loss of symbionts, the percentage symbiont loss was calculated as: 1−(6 h mean fluorescence/0 h mean fluorescence)×100, and correlated to total protein using a Pearson's correlation test.

RNA extraction and cDNA synthesis

Total RNA was extracted from each anemone using an extraction protocol described by Poole et al. (2016), with TRIzol Reagent (Invitrogen, Carlsbad, CA, USA) and an RNeasy Mini kit (Qiagen, Valencia, CA, USA). The homogenization step in this extraction method does not specifically target *S. minutum* RNA; however, it may have been extracted with the host RNA.

To assess primer specificity for *AP-SPHK* and *AP-SGPP* with the qPCR assay, we also tested amplification of *S. minutum* cDNA. Cultured *S. minutum* RNA was extracted using a different combination of protocols from Rosic and Hoegh-Guldberg (2010) and an RNeasy Mini kit (Qiagen). Briefly, 15 ml of CCMP830 cells in exponential growth phase at a concentration of 10^6 ml^{-1} was pelleted by centrifugation at 13,000 ***g*** for 5 min. The pellet was resuspended in 1.5 ml of f/2 media, transferred to a FastPrep screw-top tube (MP Biomedical, Santa Ana, CA, USA), and repelleted at 14,000 ***g*** for 30 s. The supernatant was removed and the pellet frozen in liquid nitrogen. Acid-washed 0.45–0.6 mm glass beads (Sigma-Aldrich, St Louis, MO, USA) and 0.5 ml TRIzol were added to the pellet, and placed in the FastPrep FP120 cell disruptor (MP Biomedical) at the low speed (4.0 s) for two 20 s pulses. The homogenate was then processed as described above for the anemone samples using a combination of the TRIzol protocol through phase separation followed by the RNeasy Mini kit (Qiagen).

RNA quality and quantity was assessed by gel electrophoresis and the NanoDrop ND-1000 (NanoDrop Products, Wilmington, DE, USA), respectively. Samples with a NanoDrop 260 nm/230 nm ratio less than 1.5 underwent the RNA purification protocol described by Poole et al. (2016). Each sample was then treated with the DNA-free kit (Invitrogen) or TURBO DNA-free kit (Invitrogen) to remove residual genomic DNA contamination. cDNA was synthesized using SuperScript III First-Strand Synthesis System (Invitrogen) with 500–750 ng of RNA and 50 µmol l^{-1} oligo $(dT)_{20}$ primer. Each cDNA sample was diluted to a final concentration of 300 ng μl^{-1} before use in the qPCR reactions. *Aiptasia pallida* (n=6) and CCMP830 (n=1) cDNA was tested for amplification of the symbiont-specific peridinin chlorophyll protein using previously published primers (Amar et al., 2008) following the GoTaq Flexi polymerase protocol (Promega, Madison, WI, USA).

RACE amplification of *AP-SPHK* and *AP-SGPP* sequences

Partial transcripts of *AP-SPHK* and *AP-SGPP* were identified from the *A. pallida* transcriptome (Lehnert et al., 2012) using tBLASTn with an expect value (E-value) ≤e−20 in Geneious v8.0.3 (Altschul et al., 1990; Kearse et al., 2012). The query protein sequences used were *Rattus norvegicus* SPHK1 (NCBI: ABF30968.1) and *Homo sapiens* SGPP (NCBI: CAC17772.1). To generate full-length cDNA sequences, we performed rapid amplification of the cDNA ends (RACE) using a FirstChoice RLM-RACE kit (Invitrogen) and RNA template from symbiotic *A. pallida*. Nested gene-specific primers (Table 1) were designed by hand for the 3′ and 5′ ends following the manufacturer's guidelines. Successful PCR products detected by gel electrophoresis were ligated into plasmids with the pGEM-T easy vector system (Promega) overnight at 4°C and cloned into MAX Efficiency DH5α competent cells (Invitrogen), following the manufacturer's protocol. Plasmids were purified using the QIAprep Spin Miniprep kit (Qiagen), product size verified with FastDigest *Eco*RI (Thermo Scientific, Waltham, MA, USA) or Promega *Eco*RI (Promega), and Sanger sequenced on the ABI 3730 capillary machine at the Center for Genome Research and Biocomputing at Oregon State University. Sequence products

Journal of Experimental Biology (2017) 220, 1709-1720 doi:10.1242/jeb.153858

Table 1. Oligonucleotide primers used in RACE, SNP detection and qPCR

Gene	Application	Primers
AP-SPHK	3′ end RACE	F 5′-ATG CTA GAC AGT GCG CAT CCA TCA-3′
	5′ end RACE	R 5′-ACC CAA CCA CTG ACT TTG AAC CGA-3′
	SNP detection	F 5′-TCT TGC TGG AGA ACG TCG AAC AGT-3′
		R 5′-ATG GCG CAG AGA TCC AAG TCA AGA-3′
	qPCR GOI	F 5′-ACT GCC ATC CCA GCG CAA GC-3′
		R 5′-GAC CAG CAT ACT CTG TAA CAC GCA-3′
AP-SGPP	5′ end RACE	R 5′-AAG TGC GTG CCA GAA GGG GTT GT-3′
	SNP detection	F 5′-AAT GCT GCG TGC TTC AGC GGA T-3′
		R 5′-ACG CGA TGG AGC CAT CAC AAG A-3′
	qPCR GOI	F 5′-AAT GCT GCG TGC TTC AGC GGA T-3′
		R 5′-TCC GTT AGC ATG GCC GTT TGG A-3′
Hsp90	qPCR GOI	F 5′-TCA CGC ATG AAG GAT AAC CA-3′
		R 5′-CTG GAC GGC ATA CTC ATC AA-3′

SNP, single nucleotide polymorphism; GOI, gene of interest.

from RACE were assembled with the transcriptome fragments using Geneious v8.0.3 (Kearse et al., 2012). We searched for conserved protein domains of SPHK and SGPP (Kohama et al., 1998; Mandala et al., 2000), nuclear localization sequence of SPHK2 (Igarashi et al., 2003) and transmembrane segments using the Consensus Constrained TOPology prediction web server (Dobson et al., 2015).

A. pallida and *S. minutum* genome comparisons

While this project was in process, the *A. pallida* genome (v1.0) was sequenced (Baumgarten et al., 2015). The predicted gene models from the genome were searched using the full-length transcripts of *AP-SPHK* and *AP-SGPP* (generated as described above) as BLASTx queries to identify homologs at Reef Genomics database (reefgenomics.org). Moreover, given that SPHK and SGPP proteins are highly conserved across eukaryotes, *A. pallida* sequences from this study were also compared with the *S. minutum* genome (OIST: symb_aug_v1.120123) using BLASTx with an E-value ≤e−10. DNA sequences of *AP-SPHK* and *AP-SGPP* from this study were aligned with BLAST hits from the *A. pallida* genome using MUSCLE (Edgar, 2004) or converted to predicted protein in Geneious v5.4.3 (Kearse et al., 2012) and aligned with representative proteins from *A. pallida*, *S. minutum* and mammalian model *R. norvegicus* (SPHK1: NCBI ABF30968.1; SPHK2: NCBI AAH79120.1; SGPP1: UniProt Q99P55.2; SGPP2: UniProt F1LZ44) using MUSCLE (Edgar, 2004).

Relative qPCR of *AP-SPHK*, *AP-SGPP* and *Hsp90*

Before developing the qPCR assay, the full-length transcripts from RACE amplification were surveyed for single nucleotide polymorphisms (SNPs), which have been shown to interfere with amplification and quantification of PCR products if they occur within primer annealing sites (Taris et al., 2008). SNP primers for the genes of interest *AP-SPHK* and *AP-SGPP* were designed with Primer3 software v 2.3.4 (Table 1) (Rozen and Skaletsky, 1999) and verified with cDNA from six anemones using cloning and sequencing methods described above (data not shown). The *Hsp90* gene sequence (AIPGENE3199) was recovered from the *A. pallida* genome (reefgenomics.org). For all genes, qPCR primers were designed to exclude SNPs and amplify a product ranging in size from 100 to 200 bp (Table 1). PCR products were verified through cloning and sequencing as described above.

Genes of interest were normalized to reference genes selected for stable expression during experimental treatments. Candidate reference genes included *poly-A binding protein* (*PABP*), *ribosomal large subunit 10* and *12* (*L10* and *L12*), *eukaryotic translation elongation factor 1 alpha 1* (*EEF1A1*) and *glyceraldehyde 3-phosphate dehydrogenase* (*GAPDH*); they were tested on 25 and 33°C-incubated samples at days 1 and 4 as described previously (Poole et al., 2016). Based on the stability values from GeNorm and NormFinder (Table S1), the combination of *PABP*, *L10* and *GAPDH* genes was selected as the reference genes for elevated temperature-treated anemones. After reference gene selection, cDNA from each sample was run in triplicate 20 µl reactions of 10 µl Power SYBR® Green PCR master mix (Applied Biosystems, Foster City, CA, USA), 5 µmol forward and reverse primer pair, 0.5 µl cDNA and RNase-free H_2O on the ABI Prism 7500 Real-Time PCR machine (Applied Biosystems) with standard settings and an additional melt curve. No-template, no-reverse transcriptase and no-primer controls were tested, as well as one interplate calibrator sample per plate. C_t values calculated by ABI 7500 software v2.0.6 (Applied Biosystems) with a set baseline threshold of 0.2 were imported into GenEx v5.3.7.332 (MultiD Analyses AB, Göteborg, Sweden) to adjust interplate variation and normalize expression to reference genes. The $\Delta\Delta C_t$ method (Livak and Schmittgen, 2001) was used to calculate relative quantities for each treatment group (27, 30 and 33°C) to the mean ΔC_t of 25°C samples at each time point (n=3). Relative quantities are presented on the $\log_2$ scale.

The best statistical model for *AP-SGPP* and *AP-SPHK* relative quantities was determined through Chi-square goodness of fit tests for the fixed effects of time (seven levels) and temperature (four levels: 25, 27, 30 and 33°C), and random effect of well placement. Relative quantities of *AP-SGPP* were fitted to a GLMM with the fixed effect of temperature and random effect of well placement, whereas *AP-SPHK* relative quantities were fitted to an intercept model. *Post hoc* two-tailed Student's *t*-tests were run for treated samples at each time point (n=3 anemones) compared with the time-matched non-heat-stressed control. *P*-values were adjusted for multiple-test comparisons using a Bonferroni correction. There was no evidence for the inclusion of the random effect of well placement in a GLMM model of *Hsp90* relative quantities (Chi-square goodness of fit, P>0.05). Therefore, the effect of temperature by time interaction on *Hsp90* expression was tested using a two-way ANOVA test. Differences between temperature and time points were found using Tukey's *post hoc* test. The significant threshold for all statistical tests was $P \leq 0.05$.

Lipid extraction and quantification

Two experimental trials were run for the lipid analysis. In both experiments, anemones were homogenized in 0.5 ml of 1× phosphate buffered saline (PBS) and spun at 2500 rpm for 3 min to gently pellet cellular debris and symbionts. For each sample, the supernatant was divided, with 100 µl set aside for protein quantification using a Bradford assay. In experiment 1, the remainder was transferred to a 13 mm borosilicate glass tube for lipid extraction using established protocols for lipid extraction for *A. pallida* (Bligh and Dyer, 1959; Garrett et al., 2013). An internal standard mixture was added to the lipid portion consisting of 25 ng ml^{-1} of C17-base-D-*erythro*-sphingosine-1-phosphate (C17-S1P) and 25 ng ml^{-1} of C17-base-D-*erythro*-sphingosine C17 (C17-Sph; Avanti Polar Lipids, Alabaster, AL, USA). A 1:2 chloroform:methanol mixture was added to each sample, agitated by vortexing for 20 s, and incubated at RT for 5 min. Then, equal volumes of chloroform and PBS were added to the mixture. After centrifugation at 4°C for 5 min at 3000 rpm, a two-phase separation was visible. The lower organic phase was collected in a clean glass tube and dried under gentle nitrogen stream. In experiment 2, the

Journal of Experimental Biology (2017) 220, 1709-1720 doi:10.1242/jeb.153858

remaining homogenized tissue was placed in a low-protein binding tube (Eppendorf, Hamburg, Germany) and stored at −80°C until shipped to Lipidomics Core Facility at Wayne State University (Detroit, MI, USA), where lipids were extracted. The same internal standard mix was added to the samples at a concentration of 25 ng ml^{-1}. A solvent mixture of ethyl acetate–isopropanol–water (60:30:10 v/v) was added to each sample followed by centrifugation at 6000 ***g*** to extract the lipids. The extraction was repeated twice and the organic supernatant from all three extractions was evaporated with nitrogen. In both experiments, lipid residue was dissolved in LC-MS grade methanol:water:formic acid:ammonium formate (60:40:0.2:2 mmol l^{-1} v/v), and stored at −20°C.

S1P and Sph were resolved using high-performance liquid chromatography (HPLC) on the Prominence XR system (Shimadzu, Kyoto, Japan) using a Targa C8 (5 µm, 2.1×20 mm, Higgins Analytical, Mountain View, CA, USA) column by the Lipidomics Core Facility at Wayne State University. The mobile phase consisted of a gradient between (i): methanol–water–ammonium formate–formic acid (5:95:1 mmol l^{-1}:0.2 v/v) and (ii): methanol–ammonium formate–formic acid (100:2 mmol l^{-1}:0.2 v/v) with a flow rate of 0.5 ml min^{-1}. The HPLC eluate was introduced to the ESI source of a QTRAP5500 mass analyzer (AB SCIEX, Framingham, MA, USA) in the positive ion mode and molecular ion–daughter ion transitions for each sphingolipid were detected using the multiple reaction monitoring (MRM) method. The MRM transition chromatograms were captured by Analyst v1.6.2 software (AB SCIEX) and quantified by MultiQuant software (AB SCIEX). Sample analytes that passed signal to noise thresholds and quality measures were quantified against internal standards and normalized to total protein (mg). The fold-change of each analyte was calculated as the 33°C-treated anemones referenced to the mean of the concentrations of control anemones at each respective time point. Differences in fold-changes and sphingolipid concentrations were tested with a non-parametric Kruskal–Wallis test followed by Dunn's *post hoc* test. In addition, each sample used for lipid extraction had recorded autofluorescence over the duration of the temperature treatment; therefore, the lipid concentrations could be correlated to final mean fluorescence using a Pearson's correlation test.

RESULTS

Identification of sphingosine rheostat genes in the *A. pallida* and *S. minutum* genomes

The rheostat enzymes SPHK and SGPP are highly conserved across eukaryotes, occurring in both cnidarian and dinoflagellate genomes. One *AP-SPHK* and one *AP-SGPP* gene were recovered from the *A. pallida* transcriptome (Lehnert et al., 2012) and matched BLAST queries with 43% (E-value=3e−43 to *R. norvegicus* SPHK1, NCBI: ABF30968.1) and 83% (E-value=9e−63 to *Homo sapiens* SGPP, NCBI: CAC17772.1) coverage, respectively. These partial transcripts were RACE-amplified and then searched against the *A. pallida* and *S. minutum* genomes that became available after this study began.

From the *A. pallida* genome, two putative *SPHK* (AIPGENE12769 and AIPGENE12827) and one *SGPP* (AIPGENE2150) were identified (Baumgarten et al., 2015). In mammals, slime mold, yeast and fruit flies, there are two SPHK isoenzymes, SPHK1 and SPHK2, which differ in cellular location, leading to some overlapping and opposing functions (reviewed by Maceyka et al., 2005; Alemany et al., 2007; Chan et al., 2013). It is unclear whether the two SPHK enzymes arose from a common ancestor or are the result of lineage-specific gene duplication and diversification. To determine whether the predicted gene models recovered from the genome were two distinct *SPHK* genes, the *AP-SPHK* sequence was compared with the gene models using multiple sequence alignments. A nucleotide pairwise comparison of the RACE-amplified *AP-SPHK* sequence with the genome sequences resulted in 97.9% identity to AIPGENE12769 and 58.5% identity to AIPGENE12827 (Fig. S1). For the *A. pallida* genome assembly, annotation was automated based on translated sequence similarity to the Swiss-Prot database. The transcript AIPGENE12769 that had higher similarity to the RACE-amplified sequence was annotated based on similarity to the mouse SPHK2 in Swiss-Prot (Q9JIA7). The other transcript (AIPGENE12827) was annotated by similarity to *Arabidopsis* SPHK1 in Swiss-Prot (Q8L7L1) but only matches with 32.6% identity to the Swiss-Prot sequence, mainly at the C-terminal end. Furthermore, the two genome sequences were found adjacent to one another on the same scaffold (data not shown). This arrangement can arise from segmental duplications during genome draft assembly of diploid organisms with heterozygous allele copies, especially those in highly divergent regions (Kelley and Salzberg, 2010). Given that only one transcript has been identified in the transcriptome, RACE amplification and other cnidarian resources (Table S2), we suggest that the two gene models identified in the genome originate from sequence mis-assembly rather than from gene duplication. Therefore, the results presented in this study are based on the full-length RACE-amplified *AP-SPHK* transcript available at NCBI, accession no. KY038070. To determine whether *AP-SPHK* was more similar to the cytosolic SPHK1 or membrane-bound SPHK2 identified in mammals, we compared the protein translation of AP-SPHK with *R. norvegicus* SPHK1 and SPHK2 using a multiple protein sequence alignment (Fig. S2). AP-SPHK did not share the hallmark features of membrane-bound SPHK2, which includes a 200 amino acid proline-rich insert between domains 4 and 5 (Liu et al., 2000), four transmembrane segments (Liu et al., 2000) and a nuclear localization sequence at the N-terminus (Igarashi et al., 2003) (hydropathy data not shown).

There are also two *SGPP* genes with three conserved domains (Fig. S3) (Spiegel and Milstien, 2003). We converted the RACE-amplified *AP-SGPP* transcript to protein *in silico* and compared it with the *A. pallida* genome match AIPGENE2150, *R. norvegicus* SGPP1 and SGPP2 using a multiple protein sequence alignment (Fig. S3). Pairwise identity was 96.7%, 33.2% and 31.6%, respectively. The low sequence similarity observed to the *R. norvegicus* SGPPs is comparable to the predicted homolog in oyster *Crassostrea gigas* (Timmins-Schiffman and Roberts, 2012).

In the *S. minutum* genome, one *SPHK* homolog was recovered (symbB1.v1.2.011198.t1, E-value=7e−41), but none were recovered for *SGPP* with the rat or human sequences as queries. However, using the plant *Arabidopsis thaliana* SGPP protein sequence NP_191408 as a query, two homologs from *S. minutum* (symbB1.v1.2.002394.t1, E-value=4e−32; and symbB1.v1.2.027512.t1, E-value=3e−18) were identified that contained a phosphatidic acid phosphatase type 2 domain found in *SGPP* and a larger group of lipid phosphate phosphohydrolyases. Based on protein sequence similarity, AP-SPHK and *S. minutum* SPHK share just 25.3% pairwise identity (Fig. S2). Therefore, both partners have the molecular machinery necessary to cycle S1P and Sph, but the enzymes are highly divergent at the protein level.

Heat stress alters gene expression of sphingosine rheostat enzymes

Given that homologs of *SPHK* and *SGPP* were identified in *A. pallida* and *S. minutum* genomes, we developed a host-specific

Journal of Experimental Biology (2017) 220, 1709-1720 doi:10.1242/jeb.153858

qPCR assay that excluded amplification of the symbiont enzymes. During RNA extraction, anemones had varying amounts of accompanying symbiont RNA. This contamination was confirmed with amplification of a *Symbiodinium*-specific protein, peridinin chlorophyll protein, from sample cDNA (data not shown). Therefore, we tested the specificity of the *A. pallida* qPCR primers for amplification of *S. minutum* cDNA. *AP-SPHK* qPCR primers failed to amplify a product from symbiont cDNA but *AP-SGPP* qPCR primers did amplify a product at a high mean C_t cycle of 34.208±0.35. Although a product was detected with the *AP-SGPP* qPCR primers, this amplification was shifted by 7.2 cycles from *A. pallida* cDNA expression (mean C_t=27.0.13±0.19) and therefore considered to be a non-specific PCR product. These results indicated that the qPCR primers captured host-specific expression.

To test the hypothesis that the sphingosine rheostat is part of the immediate HSR in cnidarians, relative expression of rheostat genes *AP-SPHK* and *AP-SGPP* was measured in symbiotic anemones incubated in ambient (25°C) and hyperthermal (27, 30 and 33°C) temperatures at several time points. A range of temperatures was tested over 1 week to determine thermal and temporal activation of rheostat transcription. Relative quantities of *AP-SGPP* decreased 0.8-fold in 33°C-incubated anemones, but not with more moderate elevated temperatures (GLMM conditional R^2=0.716, P=0.003; Fig. 2A). However, *AP-SGPP* expression was not downregulated over the entire time course. It significantly declined between 3 h and 1 day (*post hoc* *t*-test, 3 h: P=0.008, 6 h: P=0.003, 12 h: P=0.012, 1 day: P=0.031), began to increase by the second day and eventually exceeded control expression at 1 week (*post hoc* *t*-test, 7 days: P=0.011). In contrast, relative quantities of *AP-SPHK* did not differ between any of the four temperature treatments (linear regression R^2=0.2037, P=0.096; Fig. 2B). The *post hoc* test, however, revealed significantly decreased *AP-SPHK* expression at 12 h in 30°C and 1 day in 33°C conditions compared with ambient temperature (*post hoc* *t*-test, 12 h: P=0.002, 1 day: P=0.031). So, although there was no difference between hyperthermal temperatures in terms of *AP-SPHK* expression over time, downregulation was observed for specific time points. By the end of 1 week, an opposing expression pattern of the rheostat genes emerged, but it was not significant for *AP-SPHK* (*post hoc* *t*-test, P=0.112; Fig. 2). Overall, the relative quantities of both rheostat genes were initially downregulated with acute hyperthermal stress and then there was a shift to upregulation of *AP-SGPP* by the end of the experiment.

Rapid changes in bleaching response and *Hsp90* expression in *A. pallida*

From the range of temperatures tested, the most extreme 33°C hyperthermal treatment initiated a greater transcriptional response of the sphingosine rheostat than the intermediate hyperthermal treatments (Fig. 2). Therefore, we only compared animals incubated at ambient and 33°C in subsequent analyses. We were next interested to see how the timeline of symbiont loss and onset of a HSR of the host corresponded to changes in sphingosine rheostat expression during incubation at elevated temperature. We hypothesized that if the rheostat is driving bleaching, then changes in rheostat gene expression would occur before evidence of bleaching. Relative symbiont densities of anemones were quantified by measuring mean chlorophyll autofluorescence (Fig. 3A). At elevated temperature, there was evidence for a loss in symbiont autofluorescence over time (GLMM, conditional R^2=0.68). For each additional day, mean autofluorescence was 2.36 times lower in heat-stressed anemones compared with the controls (GLMM, P<0.001; Fig. 3B). By 1 and 4 days, the mean autofluorescence in the heat-stressed animals was 28.78±4.97% and 50±4.93% lower in the hyperthermal treatment compared with the initial mean fluorescence (Fig. 3B). At 7 days, very little additional loss (1.37%) was observed (Fig. 3B). Relative symbiont loss was variable under hyperthermal stress. Therefore, we compared the percentage symbiont loss at 6 h with total protein to see whether anemone size affected symbiont loss. No correlation was detected between symbiont loss and anemone size in either temperature

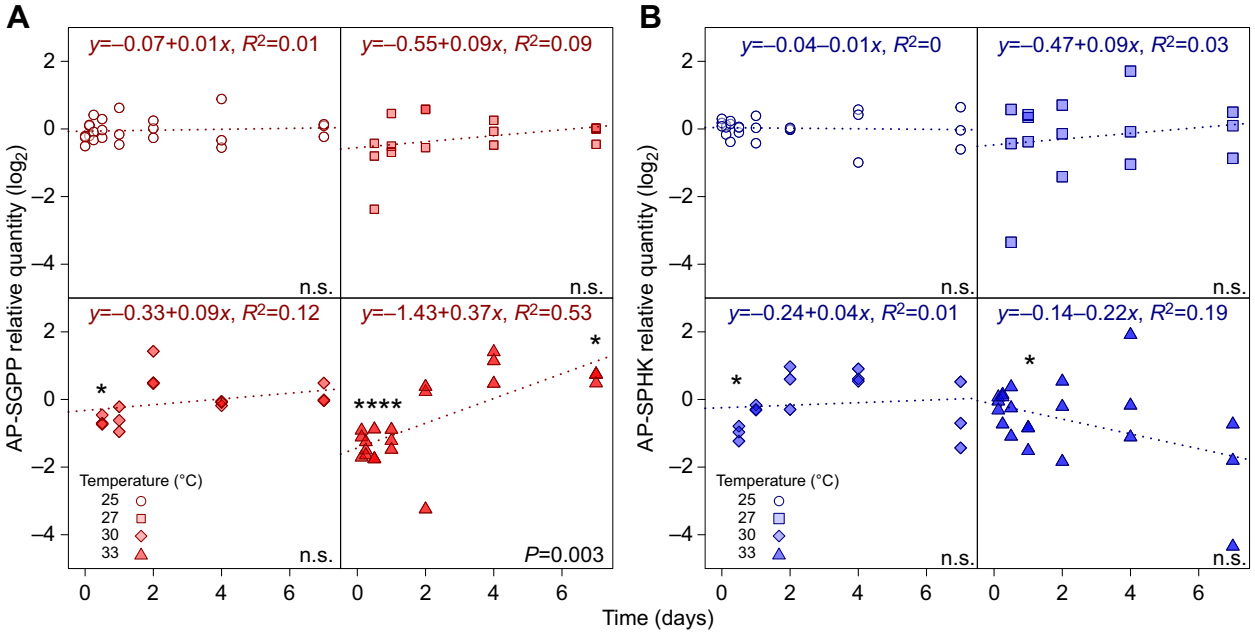

Fig. 2. *AP-SGPP* and *AP-SPHK* expression in *Aiptasia pallida* with time in elevated temperatures. Relative mRNA quantities (log_2) of (A) *AP-SGPP* and (B) *AP-SPHK* from ambient and heat-treated (27, 30 and 33°C) anemones (n=3 animals per group). The proportion of variation explained by the models (R^2) and significance (not significant, n.s., P>0.05) are displayed for each temperature. Heat-treated groups at each time point that significantly differed from their corresponding control group with *post hoc* Student's *t*-test are indicated with an asterisk, P≤0.05.

Journal of Experimental Biology

Journal of Experimental Biology (2017) 220, 1709-1720 doi:10.1242/jeb.153858

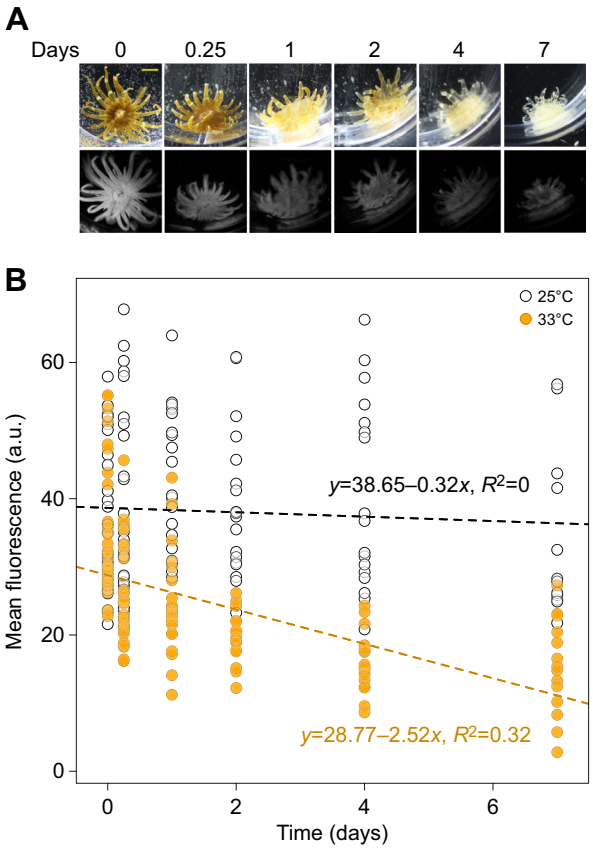

Fig. 3. Mean symbiont autofluorescence in hosts declines with elevated temperature. Anemones were incubated in either ambient (25°C) or elevated (33°C) temperature for 1 week. This was repeated in two experiments (n=16 and 20 anemones per temperature treatment in experiments 1 and 2, respectively). (A) Animals were imaged at indicated time points, with white light or with fluorescence where emission was captured with a 665 nm bandpass filter following excitation with 470 nm LED light. These photographs were taken from the same individual in the elevated temperature group. The scale bar in the top left photo is 4 mm. (B) Mean fluorescence (artificial units, a.u.) from each anemone was calculated from 10 random areas of the oral disc and fitted to GLMM regression over time. Anemones were monitored until they were killed at 6 h, 1 day, 4 days or 7 days.

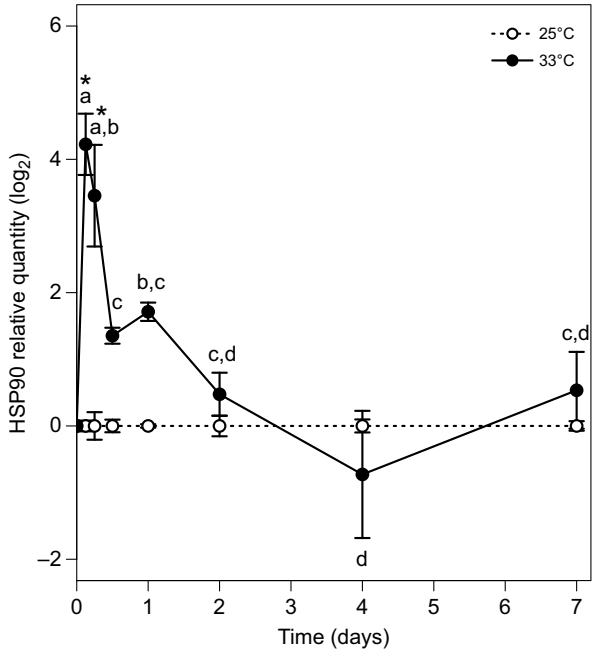

Fig. 4. Heat stress biomarker *Hsp90* expression is upregulated early during elevated temperature stress. Relative mRNA quantities ($\log_2$) of *Hsp90* with qPCR from ambient and 33°C-treated samples (n=3 anemones per group; same samples as in Fig. 2). Treatment groups were compared using a two-way ANOVA. Time points were compared with Tukey's *post hoc* test between temperatures indicated by an asterisk and within the elevated temperature treatment noted by lowercase letters. Time points that share letters were not statistically different from one another. Points represent means±s.e.m.

treatment (Pearson's correlation, 25°C correlation=−0.06 and P=0.65, and 33°C correlation=0.18 and P=0.27; Fig. S4).

To detect the onset of the HSR in *A. pallida*, we measured the gene expression of a characterized biomarker of stress in cnidarians, molecular chaperone Hsp90 (see review by Louis et al., 2017). In *A. pallida*, there was a significant interaction between temperature treatment and time on the relative quantities of *Hsp90* (two-way ANOVA, P<0.001; Fig. 4). At 3 and 6 h, the relative quantities of *Hsp90* were upregulated 4.22- and 3.45-fold, respectively, in the hyperthermal treatment compared with the time-matched controls (Tukey's *post hoc*, 3 and 6 h: P<0.001). The expression of *Hsp90* remained elevated in anemones in the hyperthermal condition between 12 h and 1 day, but this did not differ from the baseline expression at 2 and 7 days in this treatment group or the control group (Fig. 4). There was evidence for a slight downregulation of *Hsp90* expression at 4 days in the hyperthermal treatment that statistically differed from the upregulation observed between 3 h and 1 day (Fig. 4).

Sphingolipid cellular levels follow expression differences

Although transcriptional differences between rheostat genes were not observed until several days after the onset of heat stress, post-translational activation of AP-SPHK and AP-SGPP proteins could be part of the immediate HSR. We indirectly measured the enzymatic activity of rheostat enzymes by quantifying their products, S1P and Sph. Between 6 h and 4 days, Sph concentrations were lower in the heat-stressed anemones than in their corresponding controls at ambient temperature, resulting in lower lipid concentrations and fold-changes below 1 (Fig. 5A; Fig. S5A). However, the median fold-change of Sph increased by 0.77 between 6 h and 7 days (Fig. 5A; Dunn's *post hoc* test, P=0.021). Median S1P fold-change remained low throughout the experiment (Fig. 5B), but S1P concentrations at 6 h differed from those at 4 and 7 days in anemones in the hyperthermal condition (Fig. S5B; Dunn's *post hoc* test, 4 days: P=0.023 and 7 days: P=0.031).

Given that loss of symbionts varied across individuals, the severity of the hyperthermal stress on symbiosis breakdown was not uniform. More thermotolerant anemones (those with less symbiont loss) might therefore undergo regulation of sphingolipid metabolism that contributes to resistance to bleaching. To examine this, we correlated the mean fluorescence of ambient and 33°C-treated anemones to their recovered sphingolipid concentrations. At 33°C, there was no evidence that Sph or S1P concentrations were correlated with hyperthermal exposure and symbiont loss (Pearson's correlation, Sph correlation=0.23 and P=0.19, and S1P correlation=0.07 and P=0.68; Fig. 6).

DISCUSSION

We examined the activation of the sphingosine rheostat with heat stress as part of the signaling cascades involved in the cnidarian HSR and symbiosis breakdown. Our findings, summarized in Fig. 7, suggest that although the rheostat is involved in the HSR,

Journal of Experimental Biology (2017) 220, 1709-1720 doi:10.1242/jeb.153858

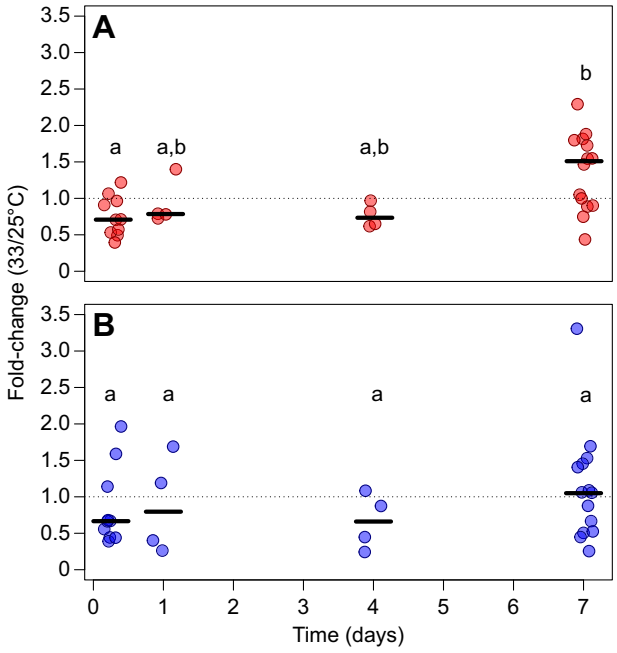

Fig. 5. Fold-change of Sph levels increases with elevated temperature stress but there is no change in S1P levels. Sphingolipid concentrations from ambient and heat-stressed anemones (n=32 anemones per treatment group: n=12 anemones for experiment 1 and n=20 anemones for experiment 2) were compared at time points with significant expression differences in *AP-SGPP* (Fig. 2). Fold-changes of Sph (A, red) and S1P (B, blue) were calculated at each time point as hyperthermal temperature over the average of the time-matched non-heat-stressed ambient group, and then analyzed with non-parametric Kruskal–Wallis test. Significance with Dunn's *post hoc* test is indicated by lowercase letters, where groups with different letters are statistically different from each other (Benjamini–Hochberg adjusted $P \leq 0.05$). Bars show the median fold-change for each metabolite for individual days.

symbiosis breakdown precedes changes in the gene expression and activity of the rheostat. Therefore, there is no evidence in this study that the rheostat directly initiates cnidarian bleaching.

The HSR dynamically alters almost all cellular processes in a highly orchestrated fashion and occurs in two response phases: acute (phase I) and chronic (phase II) (Balogh et al., 2013; Chen et al., 2013). In phase I, those processes required for immediate action including post-translational modifications of existing proteins, and rapid elevations in transcription and synthesis of Hsps and other stress-responsive proteins, coincide with the downregulation of most non-essential cellular processes (Graner et al., 2007; Morimoto, 1993). Therefore, the expression of *Hsps* is an important biomarker for phase I of the HSR in cnidarians. After 1 day of thermal stress exposure, *Hsp90* was upregulated in the corals *Orbicella faveolata* (DeSalvo et al., 2008), *Acropora millepora* larvae (Rodriguez-Lanetty et al., 2009), *Acropora palmata* (DeSalvo et al., 2010), *Acropora aspera* (Leggat et al., 2011), *Acropora tenuis* (Yuyama et al., 2012) and *Porites asteroides* (Kenkel et al., 2011). However, under chronic stress conditions, *Hsp90* was downregulated in *P. asteroides* (Kenkel et al., 2013). Following phase I, processes essential for slower, longer term acclimatization are regulated by changes in gene expression, metabolism and membrane organization as part of phase II (Balogh et al., 2013; de Nadal et al., 2011). The timing of phase II is dependent on the severity and duration of the stress and the thermal tolerance of the partners, all of which contribute to the cnidarian HSR (Hofmann and Todgham, 2010; Tchernov et al., 2004).

In *A. pallida*, *S. minutum* loss is a rapid process and is temporally associated with phase I of the HSR (Fig. 7). We observed 40% loss after 1 day at 33°C, a value within the range of other studies that noted significant symbiont pigment and density loss after acute heat stress (Detournay and Weis, 2011; Dunn et al., 2004; Gates et al., 1992; Hawkins et al., 2013; Paxton et al., 2013; Perez and Weis, 2006; Sawyer and Muscatine, 2001; Tolleter et al., 2013). This dysbiosis coincides with early upregulation of *Hsp90* expression (Fig. 7) observed in this study and elevated caspase activity, NO production and ultimately host cell death in anemones exposed to elevated temperatures from 31.5 to 33.5°C reported in other studies (Black et al., 1995; Detournay and Weis, 2011; Dunn et al., 2007; Hawkins and Davy, 2012; Paxton et al., 2013). However, not all host–symbiont combinations of *A. pallida* bleach as quickly. The *A. pallida* strain

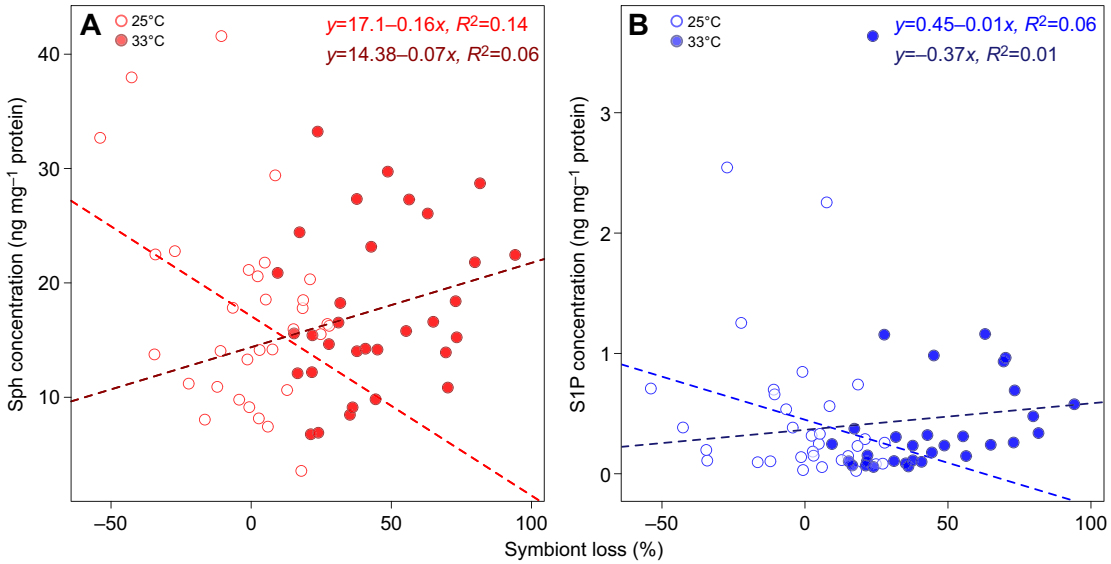

Fig. 6. Loss of symbiont autofluorescence in hosts is not correlated with sphingolipid concentration. Pearson's correlation analysis of sphingolipid (A) Sph and (B) S1P concentrations found no evidence for a relationship with symbiont loss at elevated temperature. Mean fluorescence was measured in anemones used for lipid extraction, thereby allowing for direct correlation of treatment conditions. Percentage symbiont loss was calculated as 1−(mean fluorescence final time point/mean fluorescence at day 0)×100.

Journal of Experimental Biology

Journal of Experimental Biology (2017) 220, 1709-1720 doi:10.1242/jeb.153858

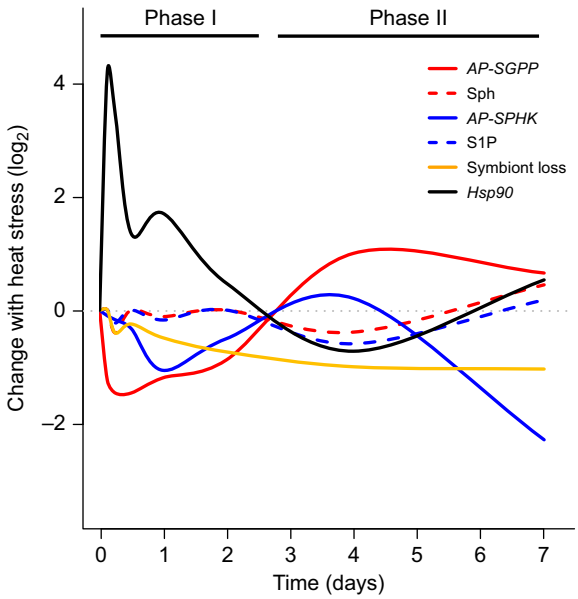

Fig. 7. Our model of the biphasic sphingosine rheostat response and symbiont loss in *A. pallida* with elevated temperature. During phase I (3 h to 2 days), *Hsp90* (black) was upregulated, symbiont density decreased by half, and the sphingosine rheostat transcriptional response and lipid levels were downregulated. After 2 days of heat treatment, *AP-SPHK* and *AP-SGPP* expression was upregulated followed by altered lipid concentrations (Sph, S1P) in phase II. Average symbiont loss was calculated as 1−average mean fluorescence at final time point at 33°C. To allow for comparisons between analyses, lipid fold-changes and average symbiont loss were converted to the $\log_2$ scale.

CC7 with *S. linucheae* (subclade A4) did not have significant symbiont loss until 7 days of hyperthermal treatment, but caspase activity was elevated as early as 2 h (Bieri et al., 2016). These differences in bleaching response could result from different thermal sensitivities of the *A. pallida* genotype, symbiont species or both.

The activity of the sphingosine rheostat, a regulator of host cell death and NO production, was not part of phase I, thereby refuting our original hypothesis. During phase I, both rheostat genes and lipid concentrations were downregulated (Fig. 7). Based on a transcriptomic study, symbiotic anemones have lower constitutive *AP-SGPP* gene expression than aposymbiotic anemones (Rodriguez-Lanetty et al., 2006). Therefore, we predict that the symbiotic *A. pallida* could have a surplus of AP-SPHK transcripts from elevated AP-SPHK expression that could be recruited to mitigate the heat-induced cellular damage before initiating a transcriptional response of the rheostat. The high sample variation in S1P concentrations at early time points suggests that some anemones had elevated AP-SPHK activity. Expression of the gene encoding the pro-apoptotic enzyme AP-SGPP and subsequent elevations in Sph concentrations were induced by longer term incubations at the highest temperature of 33°C in *A. pallida*, but not by moderately high temperatures of 27 and 30°C. In a previous study, the slow heating of *A. pallida* revealed two peaks in proteolytic activity of caspase 3 and 9, two cysteine proteases essential in apoptosis, at day 1 and 5 at the maximal temperature (33°C) (Hawkins et al., 2013).The increase in Sph between days 4 and 7 observed in this study could trigger pro-apoptotic mechanisms as part of the chronic HSR. Our results suggest that initiation of dysbiosis is part of the acute response (phase I) and sphingosine rheostat activation is part of the chronic response (phase II) in symbiotic *A. pallida* (Fig. 7).

Despite the fact that additions of exogenous S1P and Sph altered bleaching in *A. pallida* (Detournay and Weis, 2011), the endogenous rheostat examined in this study did not change during rapid bleaching in phase I. This suggests that symbiont loss is independent of sphingosine rheostat activation. Thus, the cellular programs in the host controlling initial bleaching do not appear to include the rheostat. We measured the response of the whole animal to thermal stress, but it is important to consider that the microenvironment of gastrodermal tissue where *Symbiodinium* spp. reside might be significantly different from the animal as a whole. Further investigation into the tissue-specific effects of the rheostat using single-cell expression profiling or fluorescently tagged sphingolipid localization will help reveal the involvement of sphingolipids in dysbiosis.

Other components of the sphingolipid signaling and their downstream effectors may contribute to symbiont removal and increased apoptosis or NO production during the acute HSR. An important step in the mammalian HSR is the rapid accumulation of ceramide (see Fig. 1) that precedes apoptosis in mammalian cell lines (Goldkorn et al., 1991; Jenkins et al., 2002; Nagai et al., 2011). In addition to its role in cell death, ceramide can activate eNOS leading to high NO levels (Florio et al., 2003). NO production regulates ceramide levels, synthesis and trafficking, and determines cell fate (see Fig. 1). Furthermore, Hsp90 is an allosteric enhancer of eNOS (García-Cardeña et al., 1998) and inducible NOS (Yoshida and Xia, 2003). Immunoprecipitation studies suggest the presence of similar allosteric interactions in the soft coral *Eunicea fusca* subjected to a heat stress (Ross, 2014). Pathways for ceramide production in *A. pallida* are unexplored. Future studies aimed at investigating ceramide levels and enzymes involved in accumulating ceramide will enhance our understanding of the cnidarian HSR and HSR evolution in eukaryotes.

In summary, we have shown that transcriptional activation and activity of the cnidarian sphingosine rheostat are not associated with the acute phase HSR or initiation of dysbiosis but are instead part of the longer term chronic HSR. The sphingosine rheostat could therefore be participating in longer term mechanisms of host survival under heat stress, but not a mediator of the complex mechanisms underlying symbiont removal and dysbiosis. To isolate the physiological changes of heat stress from those associated with symbiosis breakdown, other non-symbiotic model cnidarians such as the sea anemone *Nematostella vectensis* or hydrozoan *Hydra vulgaris* are good candidates for examining the role of the sphingosine rheostat in the HSR. Nevertheless, this study demonstrates a shift in the sphingosine rheostat in a symbiotic cnidarian under prolonged thermal stress toward cell death and increases our understanding of its role in an evolutionarily conserved stress response.

Acknowledgements

The authors would like to thank Dr Robert Mason, Dr Camille Paxton, Dr Angela Poole, Trevor Tivey, Jessica Flesher, Kinsey Matthews and Darian Thompson for their assistance in the execution of the study. In addition, the authors would like to thank Drs Dee Denver, John Fowler, Nathan Kirk, Eli Meyer and Barbara Taylor for their thoughtful feedback on the data analysis and manuscript.

Competing interests

The authors declare no competing or financial interests.

Author contributions

S.A.K. and V.M.W. designed the study. S.A.K. performed the data collection and analysis. S.A.K. and V.M.W. wrote the paper.

Funding

Funding was provided by the Department of Integrative Biology at Oregon State University (to S.A.K.) and by the National Science Foundation (grants IOB0919073 and IOB1529059 to V.M.W.).

Data availability

The *AP-SPHK* sequence has been deposited at NCBI, accession number KY038070.

Supplementary information

Supplementary information available online at
http://jeb.biologists.org/lookup/doi/10.1242/jeb.153858.supplemental

References

Ader, I., Brizuela, L., Bouquerel, P., Malavaud, B. and Cuvillier, O. (2008). Sphingosine kinase 1: a new modulator of hypoxia inducible factor 1α during hypoxia in human cancer cells. *Cancer Res.* **68**, 8635-8642.

Alemany, R., van Koppen, C. J., Danneberg, K., ter Braak, M. and zu Heringdorf, D. M. (2007). Regulation and functional roles of sphingosine kinases. *Naunyn Schmiedeberg Arch. Pharmacol.* **374**, 413-428.

Altschul, S. F., Gish, W., Miller, W., Myers, E. W. and Lipman, D. J. (1990). Basic local alignment search tool. *J. Mol. Biol.* **215**, 403-410.

Amar, K.-O., Douek, J., Rabinowitz, C. and Rinkevich, B. (2008). Employing of the amplified fragment length polymorphism (AFLP) methodology as an efficient population genetic tool for symbiotic cnidarians. *Mar. Biotechnol.* **10**, 350-357.

An, D., Na, C., Bielawski, J., Hannun, Y. A. and Kasper, D. L. (2011). Membrane sphingolipids as essential molecular signals for *Bacteroides* survival in the intestine. *Proc. Nat.l. Acad. Sci. USA* **108**, 4666-4671.

Balogh, G., Péter, M., Glatz, A., Gombos, I., Török, Z., Horváth, I., Harwood, J. L. and Vígh, L. (2013). Key role of lipids in heat stress management. *FEBS Lett.* **587**, 1970-1980.

Baumgarten, S., Simakov, O., Esherick, L. Y., Liew, Y. J., Lehnert, E. M., Michell, C. T., Li, Y., Hambleton, E. A., Guse, A., Oates, M. E. et al. (2015). The genome of *Aiptasia*, a sea anemone model for coral symbiosis. *Proc. Nati.l Acad. Sci. USA* **112**, 11893-11898.

Bieri, T., Onishi, M., Xiang, T., Grossman, A. R. and Pringle, J. R. (2016). Relative contributions of various cellular mechanisms to loss of algae during cnidarian bleaching. *PLoS ONE* **11**, e0152693.

Black, N. A., Voellmy, R. and Szmant, A. M. (1995). Heat shock protein induction in *Montastraea faveolata* and *Aiptasia pallida* exposed to elevated temperatures. *Biol. Bull.* **188**, 234-240.

Bligh, E. G. and Dyer, W. J. (1959). A rapid method of total lipid extraction and purification. *Can. J. Biochem. Physiol.* **37**, 911-917.

Chan, H. and Pitson, S. M. (2013). Post-translational regulation of sphingosine kinases. *Biochim. Biophys. Acta* **1831**, 147-156.

Chang, Y., Abe, A. and Shayman, J. A. (1995). Ceramide formation during heat shock: a potential mediator of alpha B-crystallin transcription. *Proc. Nat.l. Acad. Sci. USA* **92**, 12275-12279.

Chen, M.-C., Cheng, Y.-M., Sung, P.-J., Kuo, C.-E. and Fang, L.-S. (2003). Molecular identification of Rab7 (ApRab7) in *Aiptasia pulchella* and its exclusion from phagosomes harboring zooxanthellae. *Biochem. Biophys. Res. Commun.* **308**, 586-595.

Chen, M.-C., Cheng, Y.-M., Hong, M.-C. and Fang, L.-S. (2004). Molecular cloning of Rab5 (ApRab5) in *Aiptasia pulchella* and its retention in phagosomes harboring live zooxanthellae. *Biochem. Biophys. Res. Commun.* **324**, 1024-1033.

Chen, M.-C., Hong, M.-C., Huang, Y.-S., Liu, M.-C., Cheng, Y.-M. and Fang, L.-S. (2005). ApRab11, a cnidarian homologue of the recycling regulatory protein Rab11, is involved in the establishment and maintenance of the *Aiptasia* - *Symbiodinium* endosymbiosis. *Biochem. Biophys. Res. Commun.* **338**, 1607-1616.

Chen, P.-W., Fonseca, L. L., Hannun, Y. A. and Voit, E. O. (2013). Coordination of rapid sphingolipid responses to heat stress in yeast. *PLoS Comput. Biol.* **9**, e1003078.

Cuvillier, O., Pirianov, G., Kleuser, B., Vanek, P. G., Coso, O. A., Gutkind, J. S. and Spiegel, S. (1996). Suppression of ceramide-mediated programmed cell death by sphingosine-1-phosphate. *Nature* **381**, 800-803.

de Nadal, E., Ammerer, G. and Posas, F. (2011). Controlling gene expression in response to stress. *Nat. Rev. Genet.* **12**, 833-845.

Deng, X., Yin, X., Allan, R., Lu, D. D., Maurer, C. W., Haimovitz-Friedman, A., Fuks, Z., Shaham, S. and Kolesnick, R. (2008). Ceramide biogenesis is required for radiation-induced apoptosis in the germ line of *C. elegans*. *Science* **322**, 110-115.

De Palma, C., Meacci, E., Perrotta, C., Bruni, P. and Clementi, E. (2006). Endothelial nitric oxide synthase activation by tumor necrosis factor α through neutral sphingomyelinase 2, sphingosine kinase 1, and sphingosine 1 phosphate receptors: a novel pathway relevant to the pathophysiology of endothelium. *Arterioscler. Thromb. Vasc. Biol.* **26**, 99-105.

DeSalvo, M. K., Voolstra, C. R., Sunagawa, S., Schwarz, J. A., Stillman, J. H., Coffroth, M. A., Szmant, A. M. and Medina, M. (2008). Differential gene expression during thermal stress and bleaching in the Caribbean coral *Montastraea faveolata*. *Mol. Ecol.* **17**, 3952-3971.

DeSalvo, M. K., Sunagawa, S., Voolstra, C. R. and Medina, M. (2010). Transcriptomic responses to heat stress and bleaching in the elkhorn coral *Acropora palmata*. *Mar. Ecol. Prog. Ser.* **402**, 97-113.

Detournay, O. and Weis, V. M. (2011). Role of the sphingosine rheostat in the regulation of cnidarian-dinoflagellate symbioses. *Biol. Bull.* **221**, 261-269.

Dobson, L., Reményi, I. and Tusnády, G. E. (2015). CCTOP: a Consensus Constrained TOPology prediction web server. *Nucleic Acids Res.* **43**, W408-W412.

Dunn, S. R., Thomason, J. C., Le Tissier, M. D. A. and Bythell, J. C. (2004). Heat stress induces different forms of cell death in sea anemones and their endosymbiotic algae depending on temperature and duration. *Cell Death Differ.* **11**, 1213-1222.

Dunn, S. R., Schnitzler, C. E. and Weis, V. M. (2007). Apoptosis and autophagy as mechanisms of dinoflagellate symbiont release during cnidarian bleaching: every which way you lose. *Proc. R. Soc. Lond. B Biol. Sci.* **274**, 3079-3085.

Edgar, R. C. (2004). MUSCLE: multiple sequence alignment with high accuracy and high throughput. *Nucleic Acids Res.* **32**, 1792-1797.

Florio, T., Arena, S., Pattarozzi, A., Thellung, S., Corsaro, A., Villa, V., Massa, A., Diana, F., Spoto, G. and Forcella, S. (2003). Basic fibroblast growth factor activates endothelial nitric-oxide synthase in CHO-K1 cells via the activation of ceramide synthesis. *Mol. Pharmacol.* **63**, 297-310.

García-Cardeña, G., Fan, R., Shah, V., Sorrentino, R., Cirino, G., Papapetropoulos, A. and Sessa, W. C. (1998). Dynamic activation of endothelial nitric oxide synthase by Hsp90. *Nature* **392**, 821-824.

Garrett, T. A., Schmeitzel, J. L., Klein, J. A., Hwang, J. J. and Schwarz, J. A. (2013). Comparative lipid profiling of the cnidarian *Aiptasia pallida* and its dinoflagellate symbiont. *PLoS ONE* **8**, e57975.

Gates, R. D., Baghdasarian, G. and Muscatine, L. (1992). Temperature stress causes host cell detachment in symbiotic cnidarians: Implications for coral bleaching. *Biol. Bull.* **182**, 324-332.

Goldstein, B. and King, N. (2016). The future of cell biology: emerging model organisms. *Trends Cell Biol.* **26**, 818-824.

Goldkorn, T., Dressler, K. A., Muindi, J., Radin, N. S., Mendelsohn, J., Menaldino, D., Liotta, D. and Kolesnick, R. N. (1991). Ceramide stimulates epidermal growth factor receptor phosphorylation in A431 human epidermoid carcinoma cells. Evidence that ceramide may mediate sphingosine action. *J. Biol. Chem.* **266**, 16092-16097.

Gomez-Brouchet, A., Pchejetski, D., Brizuela, L., Garcia, V., Altie, M.-F., Maddelein, M.-L., Delisle, M.-B. and Cuvillier, O. (2007). Critical role for sphingosine kinase-1 in regulating survival of neuroblastoma cells exposed to amyloid-β peptide. *Mol. Pharmacol.* **72**, 341-349.

Goulet, T. L., Cook, C. B. and Goulet, D. (2005). Effect of short-term exposure to elevated temperatures and light levels on photosynthesis of different host-symbiont combinations in the Aiptasia pallida/Symbiodinium symbiosis. *Limnol. Oceanogr.* **50**, 1490-1498.

Grajales, A. and Rodriguez, E. (2014). Morphological revision of the genus *Aiptasia* and the family Aiptasiidae (Cnidaria, Actiniaria, Metridioidea). *Zootaxa* **3826**, 55-100.

Grajales, A. and Rodríguez, E. (2016). Elucidating the evolutionary relationships of the Aiptasiidae, a widespread cnidarian–dinoflagellate model system (Cnidaria: Anthozoa: Actiniaria: Metridioidea). *Mol. Phylogenet. Evol.* **94**, 252-263.

Graner, M. W., Cumming, R. I. and Bigner, D. D. (2007). The heat shock response and chaperones/heat shock proteins in brain tumors: surface expression, release, and possible immune consequences. *J. Neurosci.* **27**, 11214-11227.

Guillard, R. R. L. and Ryther, J. H. (1962). Studies of marine planktonic diatoms I. *Cyclotella nana* Hustedt and *Detonula confervacea* Cleve. *Can. J. Microbiol.* **8**, 229-239.

Hawkins, T. D. and Davy, S. K. (2012). Nitric oxide production and tolerance differ among *Symbiodinium* types exposed to heat stress. *Plant Cell Physiol.* **53**, 1889-1898.

Hawkins, T. D., Bradley, B. J. and Davy, S. K. (2013). Nitric oxide mediates coral bleaching through an apoptotic-like cell death pathway: evidence from a model sea anemone-dinoflagellate symbiosis. *FASEB J.* **27**, 4790-4798.

Hawkins, T. D., Krueger, T., Becker, S., Fisher, P. L. and Davy, S. K. (2014). Differential nitric oxide synthesis and host apoptotic events correlate with bleaching susceptibility in reef corals. *Coral Reefs* **33**, 141-153.

Hemond, E. M., Kaluziak, S. T. and Vollmer, S. V. (2014). The genetics of colony form and function in Caribbean Acropora corals. *BMC Genomics* **15**, 1133.

Henikoff, S. and Henikoff, J. G. (1992). Amino acid substitution matrices from protein blocks. *Proc. Natl. Acad. Sci. USA* **89**, 10915-10919.

Heung, L. J., Luberto, C. and Del Poeta, M. (2006). Role of sphingolipids in microbial pathogenesis. *Infect. Immun.* **74**, 28-39.

Hoegh-Guldberg, O., Mumby, P. J., Hooten, A. J., Steneck, R. S., Greenfield, P., Gomez, E., Harvell, C. D., Sale, P. F., Edwards, A. J., Caldeira, K. et al. (2007). Coral reefs under rapid climate change and ocean acidification. *Science* **318**, 1737-1742.

Hofmann, G. E. and Todgham, A. E. (2010). Living in the now: physiological mechanisms to tolerate a rapidly changing environment. *Annu. Rev. Physiol.* **72**, 127-145.

Igarashi, N., Okada, T., Hayashi, S., Fujita, T., Jahangeer, S. and Nakamura, S.-i. (2003). Sphingosine kinase 2 is a nuclear protein and inhibits DNA synthesis. *J. Biol. Chem.* **278**, 46832-46839.

Journal of Experimental Biology

Jenkins, G. M., Richards, A., Wahl, T., Mao, C., Obeid, L. and Hannun, Y. (1997). Involvement of yeast sphingolipids in the heat stress response of *Saccharomyces cerevisiae*. *J. Biol. Chem.* **272**, 32566-32572.
Jenkins, G. M., Cowart, L. A., Signorelli, P., Pettus, B. J., Chalfant, C. E. and Hannun, Y. A. (2002). Acute activation of *de novo* sphingolipid biosynthesis upon heat shock causes an accumulation of ceramide and subsequent dephosphorylation of SR proteins. *J. Biol. Chem.* **277**, 42572-42578.
Kawamura, H., Tatei, K., Nonaka, T., Obinata, H., Hattori, T., Ogawa, A., Kazama, H., Hamada, N., Funayama, T. and Sakashita, T. (2009). Ceramide induces myogenic differentiation and apoptosis in *Drosophila* Schneider cells. *J. Radiat. Res.* **50**, 161-169.
Kearse, M., Moir, R., Wilson, A., Stones-Havas, S., Cheung, M., Sturrock, S., Buxton, S., Cooper, A., Markowitz, S. and Duran, C. (2012). Geneious Basic: an integrated and extendable desktop software platform for the organization and analysis of sequence data. *Bioinformatics* **28**, 1647-1649.
Kelley, D. R. and Salzberg, S. L. (2010). Detection and correction of false segmental duplications caused by genome mis-assembly. *Genome Biol.* **11**, R28.
Kenkel, C. D., Aglyamova, G., Alamaru, A., Bhagooli, R., Capper, R., Cunning, R., deVillers, A., Haslun, J. A., Hédouin, L., Keshavmurthy, S. et al. (2011). Development of gene expression markers of acute heat-light stress in reef-building corals of the genus *Porites*. *PLoS ONE* **6**, e26914.
Kenkel, C. D., Meyer, E. and Matz, M. V. (2013). Gene expression under chronic heat stress in populations of the mustard hill coral (*Porites astreoides*) from different thermal environments. *Mol. Ecol.* **22**, 4322-4334.
Kohama, T., Olivera, A., Edsall, L., Nagiec, M. M., Dickson, R. and Spiegel, S. (1998). Molecular cloning and functional characterization of murine sphingosine kinase. *J. Biol. Chem.* **273**, 23722-23728.
Lanterman, M. M. and Saba, J. D. (1998). Characterization of sphingosine kinase (SK) activity in *Saccharomyces cerevisiae* and isolation of SK-deficient mutants. *Biochem. J.* **332**, 525-531.
Leggat, W., Seneca, F., Wasmund, K., Ukani, L., Yellowlees, D. and Ainsworth, T. D. (2011). Differential responses of the coral host and their algal symbiont to thermal stress. *PLoS ONE* **6**, e26687.
Lehnert, E. M., Burriesci, M. S. and Pringle, J. R. (2012). Developing the anemone *Aiptasia* as a tractable model for cnidarian-dinoflagellate symbiosis: the transcriptome of aposymbiotic *A. pallida*. *BMC Genomics* **13**, 271.
Lesser, M. P. (1996). Elevated temperatures and ultraviolet radiation cause oxidative stress and inhibit photosynthesis in symbiotic dinoflagellates. *Limnol. Oceanogr.* **41**, 271-283.
Le Stunff, H., Milstien, S. and Spiegel, S. (2004). Generation and metabolism of bioactive sphingosine-1-phosphate. *J. Cell. Biochem.* **92**, 882-e899.
Liu, H., Sugiura, M., Nava, V. E., Edsall, L. C., Kono, K., Poulton, S., Milstien, S., Kohama, T. and Spiegel, S. (2000). Molecular cloning and functional characterization of a novel mammalian sphingosine kinase type 2 isoform. *J. Biol. Chem.* **275**, 19513-19520.
Livak, K. J. and Schmittgen, T. D. (2001). Analysis of relative gene expression data using real-time quantitative PCR and the $2^{-\Delta\Delta CT}$ method. *Methods* **25**, 402-408.
Louis, Y. D., Bhagooli, R., Kenkel, C. D., Baker, A. C. and Dyall, S. D. (2017). Gene expression biomarkers of heat stress in scleractinian corals: Promises and limitations. *Comp. Biochem. Physiol C Toxicol. Pharmacol.* **191**, 63-77.
Maceyka, M., Payne, S. G., Milstien, S. and Spiegel, S. (2002). Sphingosine kinase, sphingosine-1-phosphate, and apoptosis. *Biochim. Biophys. Acta* **1585**, 193-201.
Maceyka, M., Sankala, H., Hait, N. C., Le Stunff, H., Liu, H., Toman, R., Collier, C., Zhang, M., Satin, L. S., Merrill, A. H. et al. (2005). SphK1 and SphK2, sphingosine kinase isoenzymes with opposing functions in sphingolipid metabolism. *J. Biol. Chem.* **280**, 37118-37129.
Maceyka, M., Milstien, S. and Spiegel, S. (2007). Shooting the messenger: oxidative stress regulates sphingosine-1-phosphate. *Circ. Res.* **100**, 7-9.
Mandala, S. M., Thornton, R., Tu, Z., Kurtz, M. B., Nickels, J., Broach, J., Menzeleev, R. and Spiegel, S. (1998). Sphingoid base 1-phosphate phosphatase: a key regulator of sphingolipid metabolism and stress response. *Proc. Natl. Acad. Sci. USA* **95**, 150-155.
Mandala, S. M., Thornton, R., Galve-Roperh, I., Poulton, S., Peterson, C., Olivera, A., Bergstrom, J., Kurtz, M. B. and Spiegel, S. (2000). Molecular cloning and characterization of a lipid phosphohydrolase that degrades sphingosine-1-phosphate and induces cell death. *Proc. Natl. Acad. Sci. USA* **97**, 7859-7864.
Mao, C., Saba, J. and Obeid, L. (1999). The dihydrosphingosine-1-phosphate phosphatases of *Saccharomyces cerevisiae* are important regulators of cell proliferation and heat stress responses. *Biochem. J.* **342**, 667-675.
McGinty, E. S., Pieczonka, J. and Mydlarz, L. D. (2012). Variations in reactive oxygen release and antioxidant activity in multiple *Symbiodinium* types in response to elevated temperature. *Microb. Ecol.* **64**, 1000-1007.
Morimoto, R. (1993). Cells in stress: transcriptional activation of heat shock genes. *Science* **259**, 1409.
Nagai, K.-i., Takahashi, N., Moue, T. and Niimura, Y. (2011). Alteration of fatty acid molecular species in ceramide and glucosylceramide under heat stress and expression of sphingolipid-related genes. *Adv. Biol. Chem.* **1**, 35-48.
Olivera, A. and Spiegel, S. (2001). Sphingosine kinase: a mediator of vital cellular functions. *Prostaglandins Other Lipid Mediat.* **64**, 123-134.
Paxton, C. W., Davy, S. K. and Weis, V. M. (2013). Stress and death of cnidarian host cells play a role in cnidarian bleaching. *J. Exp. Biol.* **216**, 2813-2820.
Pchejetski, D., Kunduzova, O., Dayon, A., Calise, D., Seguelas, M.-H., Leducq, N., Seif, I., Parini, A. and Cuvillier, O. (2007). Oxidative stress–dependent sphingosine kinase-1 inhibition mediates monoamine oxidase A–associated cardiac cell apoptosis. *Circ. Res.* **100**, 41-49.
Perez, S. and Weis, V. (2006). Nitric oxide and cnidarian bleaching: an eviction notice mediates breakdown of a symbiosis. *J. Exp. Biol.* **209**, 2804-2810.
Perrotta, C., De Palma, C. and Clementi, E. (2008). Nitric oxide and sphingolipids: mechanisms of interaction and role in cellular pathophysiology. *Biol. Chem.* **389**, 1391-1397.
Poole, A. Z., Kitchen, S. A. and Weis, V. M. (2016). The role of complement in cnidarian-dinoflagellate symbiosis and immune challenge in the sea anemone *Aiptasia pallida*. *Front. Microbiol.* **7**, 519.
Rasband, W. (1997-2015). *ImageJ. Bethesda*. Maryland, USA: U. S. National Institutes of Health.
Ren, J., Wen, L., Gao, X., Jin, C., Xue, Y. and Yao, X. (2009). DOG 1.0: illustrator of protein domain structures. *Cell Res.* **19**, 271-273.
Richier, S., Sabourault, C., Courtiade, J., Zucchini, N., Allemand, D. and Furla, P. (2006). Oxidative stress and apoptotic events during thermal stress in the symbiotic sea anemone, *Anemonia viridis*. *FEBS J.* **273**, 4186-4198.
Rodriguez-Lanetty, M., Phillips, W. S. and Weis, V. M. (2006). Transcriptome analysis of a cnidarian-dinoflagellate mutualism reveals complex modulation of host gene expression. *BMC Genomics* **7**, 23.
Rodriguez-Lanetty, M., Harii, S. and Hoegh-Guldberg, O. V. E. (2009). Early molecular responses of coral larvae to hyperthermal stress. *Mol. Ecol.* **18**, 5101-5114.
Rosic, N. N. and Hoegh-Guldberg, O. (2010). A method for extracting a high-quality RNA from *Symbiodinium* sp. *J. Appl. Phycol.* **22**, 139-146.
Ross, C. (2014). Nitric oxide and heat shock protein 90 co-regulate temperature-induced bleaching in the soft coral *Eunicea fusca*. *Coral Reefs* **33**, 513-522.
Rozen, S. and Skaletsky, H. (1999). Primer3 on the WWW for general users and for biologist programmers. In *Bioinformatics Methods and Protocols* (ed. S. Misener and S. A. Krawetz) pp. 365-386. Heidelberg: Springer.
Sawyer, S. J. and Muscatine, L. (2001). Cellular mechanisms underlying temperature-induced bleaching in the tropical sea anemone A*iptasia pulchella*. *J. Exp. Biol.* **204**, 3443-3456.
Spiegel, S. and Milstien, S. (2003). Sphingosine-1-phosphate: an enigmatic signaling lipid. *Nat. Rev. Mol. Cell Biol.* **4**, 397-407.
Starcevic, A., Dunlap, W. C., Cullum, J., Shick, J. M., Hranueli, D. and Long, P. F. (2010). Gene expression in the scleractinian *Acropora microphthalma* exposed to high solar irradiance reveals elements of photoprotection and coral bleaching. *PLoS ONE* **5**, e13975.
Steinberg, B. E. and Grinstein, S. (2008). Pathogen destruction versus intracellular survival: the role of lipids as phagosomal fate determinants. *J. Clin. Investig.* **118**, 2002-2011.
Sunagawa, S., Choi, J., Forman, H. J. and Medina, M. (2008). Hyperthermic stress-induced increase in the expression of glutamate-cysteine ligase and glutathione levels in the symbiotic sea anemone Aiptasia pallida. *Comp. Biochem. Physiol. B Biochem. Mol. Biol.* **151**, 133-138.
Taris, N., Lang, R. P. and Camara, M. D. (2008). Sequence polymorphism can produce serious artefacts in real-time PCR assays: hard lessons from Pacific oysters. *BMC Genomics* **9**, 234.
Tchernov, D., Gorbunov, M. Y., de Vargas, C., Yadav, S. N., Milligan, A. J., Häggblom, M. and Falkowski, P. G. (2004). Membrane lipids of symbiotic algae are diagnostic of sensitivity to thermal bleaching in corals. *Proc. Natl. Acad. Sci. USA* **101**, 13531-13535.
Timmins-Schiffman, E. and Roberts, S. (2012). Characterization of genes involved in ceramide metabolism in the Pacific oyster (*Crassostrea gigas*). *BMC Res. Notes* **5**, 502.
Tolleter, D., Seneca, F. O., DeNofrio, J. C., Krediet, C. J., Palumbi, S. R., Pringle, J. R. and Grossman, A. R. (2013). Coral bleaching independent of photosynthetic activity. *Curr. Biol.* **23**, 1782-1786.
van Brocklyn, J. R. and Williams, J. B. (2012). The control of the balance between ceramide and sphingosine-1-phosphate by sphingosine kinase: oxidative stress and the seesaw of cell survival and death. *Comp. Biochem. Physiol. B Biochem. Mol. Biol.* **163**, 26-36.
Venn, A. A., Loram, J. E. and Douglas, A. E. (2008). Photosynthetic symbioses in animals. *J. Exp. Bot.* **59**, 1069-1080.
Warner, M. E., Fitt, W. K. and Schmidt, G. W. (1996). The effects of elevated temperature on the photosynthetic efficiency of zooxanthellae *in hospite* from four different species of reef coral: a novel approach. *Plant Cell Environ.* **19**, 291-299.
Weis, V. M. (2008). Cellular mechanisms of Cnidarian bleaching: stress causes the collapse of symbiosis. *J. Exp. Biol.* **211**, 3059-3066.

Weis, V. M., Davy, S. K., Hoegh-Guldberg, O., Rodriguez-Lanetty, M. and Pringle, J. R. (2008). Cell biology in model systems as the key to understanding corals. *Trends Ecol. Evol.* **23**, 369-376.

Yabu, T., Imamura, S., Yamashita, M. and Okazaki, T. (2008). Identification of Mg2+-dependent neutral sphingomyelinase 1 as a mediator of heat stress-induced ceramide generation and apoptosis. *J. Biol. Chem.* **283**, 29971-29982.

Yoshida, M. and Xia, Y. (2003). Heat shock protein 90 as an endogenous protein enhancer of inducible nitric-oxide synthase. *J. Biol. Chem.* **278**, 36953-36958.

Yuyama, I., Harii, S. and Hidaka, M. (2012). Algal symbiont type affects gene expression in juveniles of the coral *Acropora tenuis* exposed to thermal stress. *Mar. Environ. Res.* **76**, 41-47.